

Highly Variable Apparent Speed in the Quasar 3C 279

S.G. Jorstad^{1,2} and A.P. Marscher¹

¹ Inst. for Astrophysical Research, Boston Univ. 725 Commonwealth Ave. Boston MA, 02215 USA

² Sobolev Astronomical Inst., St. Petersburg State Univ., 28 Universitetskij prospect, St. Petersburg, 198504 Russia

Abstract. We report results of monthly observations of the quasar 3C 279 with the VLBA at 43 GHz from May 2001 to July 2004. The monitoring, combined with previously published data, reveals a significant change in apparent speed and in projected position angle of the inner jet of the quasar. We estimate the Doppler factor of superluminal knots based on their VLBI properties. The variations in the Doppler factor correlate with the X-ray light curve of the quasar, which suggests a modulation of the X-ray variability by the jet activity. Using derived Doppler factors and apparent speeds, we compute the Lorentz factor and the viewing angle of superluminal knots. Both parameters vary significantly in a manner that we interpret as the result of hydrodynamical instabilities in the jets. However, a jet precession model with period ~ 31 yr might explain the general observed behavior as well.

Key words. quasar – 3C279 – jet

1. Introduction

The quasar 3C 279 ($z=0.538$) was the first radio source found to have a superluminal apparent speed ($\beta_{\text{app}} > 10c$ Cohen et al. 1979; Cotton et al. 1979; Porcas 1981). Since then the radio jet of the quasar has been studied intensively at different wavelengths (Pauliny-Toth et al. 1981; Unwin et al. 1989; Wehrle et al. 2001; Jorstad et al. 2001a; Homan et al. 2003; Kellermann et al. 2004; Jorstad et al. 2004) and shows a wide range of proper motions of superluminal features, from ~ 1 mas yr^{-1} to 0.12 mas yr^{-1} . In the early 1990s the quasar was found to be

a strong and variable γ -ray source (Hartman et al. 1992). This has initiated a number of multi-frequency campaigns (e.g. Wehrle et al. 1998; Hartman et al. 2001; Marscher et al. 2004) that reveal a good correlation between γ -ray and X-ray and between X-ray and optical emission. The γ -ray-X-ray variations are simultaneous within 1 day, while optical flares lead X-ray flares by a few days. In addition, a connection between the radio jet activity and γ -ray flares has been found for γ -ray blazars (Jorstad et al. 2001b). These findings suggest an inverse-Compton origin of the high-energy emission involving relativistic electrons in the radio jets (e.g., Sokolov et al. 2004), and place the variable high energy emission inside the radio jet. The latter implies that the variability of the quasar across the electromagnetic spectrum

Send offprint requests to: S.G. Jorstad

Correspondence to: IAR 725 Commonwealth Ave. Boston MA, 02215 USA

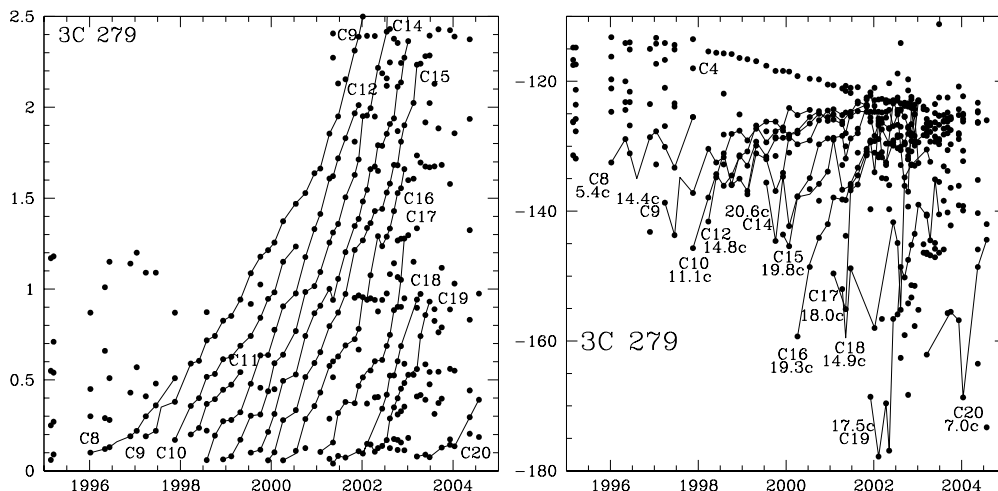


Fig. 1. Left panel: Separations of components from the core vs. time. Right panel: Projected position angle of components vs. time. Broken lines indicate identification of components across epochs. On the right panel, the apparent speed of each knot is given near the label of the knot. The uncertainty of the apparent speed does not exceed 1% of its value.

is a consequence of changes in the jet parameters. In this context, intensive VLBI monitoring at high radio frequencies, which allows us to look at the base of the jet where the high energy emission is most likely produced, plays a major role in defining the evolution of the jet parameters.

2. Observations

We have been performing monthly observations of the quasar 3C 279 with the Very Long Baseline Array (VLBA) at 43 GHz from May 2001 until the present. We have reduced the data in the same manner as in Jorstad et al. (2004). The images are modeled by circular Gaussian components using the task MODELFIT of the package DIFMAP (Shepherd 1997) to represent the jet emission at each epoch as a sequence of knots characterized by flux density, size, and distance and position relative to the map center. These data, along with the results obtained by Wehrle et al. (2001); Jorstad et al. (2001a), and Jorstad et al. (2004), form a uniform set of component parameters at 43 GHz from January 1995 to July 2004.

3. Superluminal Knots

Figure 1 shows the separation of components from the core vs. time as well as the temporal evolution of projected position angles of the features. Broken lines identify components across epochs (labeling of knots follows Wehrle et al. 2001). This identification is the most consistent according to flux variability, projected position angle in the jet, and size of features. Each component is traced at all available epochs from the extrapolated time of ejection until its disappearance from the 43 GHz maps. Since April 2001 we have continued to observe components *C9*, *C12*, *C13*, *C14*, *C15*, and *C16* detected in Jorstad et al. (2004), and see four new knots, *C17*, *C18*, *C19*, and *C20*, ejected later. Apparent speeds of the components are indicated in Figure 1 (right panel). They are calculated using the cosmological parameters $\Omega_m = 0.3$, $\Omega_\Lambda = 0.7$, and $H_0 = 70 \text{ km s}^{-1} \text{ Mpc}^{-1}$ for ballistic motion. All knots (besides *C8*) show the same pattern of trajectory: a change of the projected position angle from a south-western direction near the core to a western direction down the jet. Figure 1 shows an increase of the apparent speed from

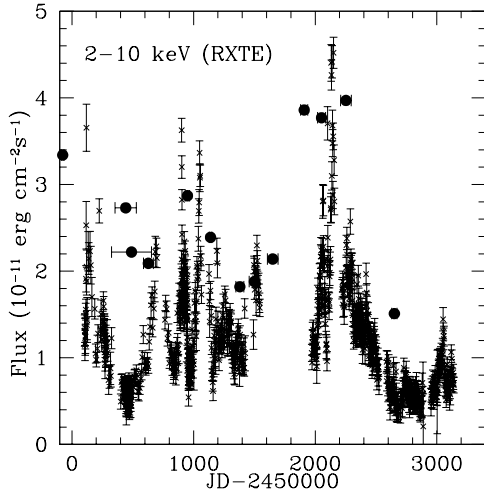


Fig. 2. RXTE light curve of 3C 279 (crosses). The filled circles show Doppler factors of jet components (divided by a factor of 10) vs. time of superluminal ejections.

$\sim 5c$ to $\sim 21c$ and then a decrease to $7c$. A similar high apparent speed ($\beta_{\text{app}} \sim 15c$) has been detected by Cotton et al. (1979) for component C1 ejected at epoch ~ 1968 . This suggests precession of the jet with Lorentz factor $\Gamma \sim 21$ and period of precession ~ 31 yr. A precessing jet model for 3C 279 has been considered by Abraham & Carrara (1998), however the observed apparent speed is significantly different than the model predicts. Although a precession model might explain the observed variations in apparent speed and trajectory of superluminal knots, two or more cycles are needed to confirm its reality. In this context, a precession period ~ 31 yr predicts a minimum in apparent speed of the jet flow in 2007 similar to the apparent speed of component C3 found by Unwin et al. (1989). This should be tested by future observations.

Figure 1 shows some features that do not move significantly, e.g., the locus of points at ~ 1 mas in 2001 and another at ~ 1.7 mas in 2003. These features have characteristics of trailing shocks that form in the interaction between major disturbances propagating down the jet and the underlying flow (Agudo et al. 2001). They all have the same lifetimes (~ 1 yr

in the observer frame) that could, for example, correspond to the time required for the underlying jet flow to restore a balance between the external and internal pressures after the passage of a superluminal knot.

Figure 1 (right panel) shows the evolution of the position angle of knot C4 located ~ 3 mas from the core and moving at an average apparent speed $\sim 10c$. The component experiences a change of trajectory that focuses its path into the direction of the inner jet, $\sim -125^\circ$. As was found by Homan et al. (2003), the new direction of motion is accompanied by acceleration of the knot. Our data confirm these findings.

4. Discussion of the Jet Parameters

Our intensive monitoring provides well-sampled light curves of individual components. Using these light curves we define the time scale of variability for each component as $\Delta t_{\text{var}} = dt / \ln(S_{\text{max}}/S_{\text{min}})$ (Burbidge, Jones, & O'Dell 1974), where S_{max} and S_{min} are the measured maximum and minimum flux densities, respectively, and dt is the time in years between epochs corresponding to S_{max} and S_{min} . If we assume that the variability timescale corresponds to the light-travel time across the knot, then the variability Doppler factor can be defined as:

$$\delta_{\text{var}} = \frac{s D}{c \Delta t_{\text{var}} (1+z)}, \quad (1)$$

where D is the luminosity distance and s is the angular size of the component, equal to $1.6a$ for gaussian FWHM a measured at the epoch of maximum flux.

Figure 2 shows the X-ray light curves of 3C 279 obtained with the Rossi X-ray Timing Explorer (see Marscher, this proceedings) and scaled Doppler factors of superluminal components vs. time of ejection. Variations of δ correspond to the changes in overall flux level of the X-ray light curve very well. This implies that the variable X-ray emission is produced in the jet, very close to the VLBI core where superluminal components are thought to be born.

Estimates of apparent speed and Doppler factor allow us to obtain the Lorentz factor,

Table 1. Parameters of Jet Components

Comp.	δ	Γ	Φ°
C8	33	17	0.5
C9	27	18	1.7
C10	22	14	2.1
C11	21	13	2.2
C12	29	18	1.6
C13	24	19	2.3
C14	18	21	3.1
C15	19	20	3.1
C16	21	19	2.7
C17	39	24	1.1
C18	38	22	1.0
C19	40	24	1.1
C20	15	9	2.9

Γ , and viewing angle, Φ , for each superluminal knot. These parameters are given in Table 1. Table 1 shows that both the Lorentz factor and the viewing angle of components vary significantly and that the variations have rather random character. These can be produced as the result of magnetohydrodynamical instabilities in accretion disk-jet driven systems (e.g., Hardee & Rosen 1999). However, the long-term variability of the quasar on time scales >10 yrs might be governed by precession of the jet. Most likely both mechanisms operate, so that the Doppler factor can be as high as 40 and the Lorentz factor can exceed 20, varying on timescales as short as a few months. These parameters agree with the high amplitude variability of the quasar from radio wavelengths to γ -ray energies.

Acknowledgements. This research is based on work supported by the National Science Foundation under grant AST-0406865. The VLBA is a facility of the National Radio Astronomy Observatory, operated

by Associated Universities Inc. under cooperative agreement with the National Science Foundation.

References

- Abraham, Z. & Carrara, E. A. 1998, ApJ 496, 172
- Agudo, I., et al. 2001, ApJ 549, L183
- Burbidge, G. R., Jones, T. W., & O'Dell, S. L. 1974, ApJ 193, 43
- Cohen, M. H., et al. 1971, ApJ 170, 207
- Cotton, W. D., et al. 1979, ApJ 225, L115
- Hardee, P. E. & Rosen, A. 1999, ApJ 524, 650
- Hartman, R. C., et al. 1992, ApJ 385, L1
- Hartman, R. C., et al. 2001, ApJ 558, 583
- Homan, D. C., et al. 2003, ApJ 589, L9
- Jorstad, S. G., et al. 2001, ApJS 134, 181
- Jorstad, S. G., et al. 2001, ApJ 556, 738
- Jorstad, S. G., et al. 2004, AJ 127, 3115
- Kellermann, K. I., et al. 2004, ApJ 609, 539
- Marscher, A. P., et al. 2004, in X-Ray Timing 2003: Rossi and Beyond, eds. P. Kaaret, F.K. Lamb, & J.H. Swank, AIP Conf. Ser. 714, 167
- Pauliny-Toth, I. I. K., et al. 1981, AJ 86, 371
- Porcas, R. W. 1981, in Superluminal Radio Sources, eds. J.A. Zensus & T.J. Pearson, (Cambridge Univ. Press), 12
- Shepherd, M. C. 1997, in Astronomical Data Analysis Software and Systems VI, eds. G. Hunt & H. E. Payne (San Francisco: ASP), ASP Conf. Proc. 125, 77
- Sokolov, A. S., Marscher, A. P., & McHardy, I. 2004, ApJ 613, 725
- Unwin, S. C., et al. 1998, ApJ 340, 117
- Wehrle, A. E., et al. 1998, ApJ 497, 178
- Wehrle, A. E., et al. 2001, ApJS 133, 297